



Original Article

Synthesis characterization and morphological study of $\text{Fe}_3\text{O}_4@\text{SiO}_2$ Core-Shell Nanoparticles

S. P. Gawali¹ D.V. Mane²

¹School of Science, Yashwantrao Chavan Maharashtra open University, Nashik, Maharashtra – India, ^bDepartment of Chemistry, Sundar Rao More Arts, Commerce and Science College, Poladpur, Raigad, India

²Former Regional Director, YCMOU Nashik India. Department of Chemistry, Shri Chhatrapati Shivaji College Omerga, Dharashiv India

Abstract

Manuscript ID:
RIGJAAR-2025-021255

ISSN: 2998-4459
Volume 2
Issue 12
Pp. 274-281
December 2025

Submitted: 16 Nov. 2025
Revised: 22 Nov. 2025
Accepted: 25 Dec. 2025
Published: 31 Dec. 2025

Correspondence Address:
S. P. Gawali
School of Science, Yashwantrao Chavan Maharashtra open University, Nashik, Maharashtra – India, ^bDepartment of Chemistry, Sundar Rao More Arts, Commerce and Science College, Poladpur, Raigad, India
Email: spgawali1986@gmail.com

Quick Response Code:



Web. <https://rlgjaar.com>



DOI: [10.5281/zenodo.18144900](https://doi.org/10.5281/zenodo.18144900)

DOI Link:
<https://doi.org/10.5281/zenodo.18144900>



Creative Commons



Creative Commons (CC BY-NC-SA 4.0)

This is an open access journal, and articles are distributed under the terms of the [Creative Commons Attribution-NonCommercial-ShareAlike 4.0 International](#) Public License, which allows others to remix, tweak, and build upon the work noncommercially, as long as appropriate credit is given and the new creations are licensed under the identical terms.

How to cite this article:

Gawali, S. P., & Mane, D. V. (2025). Synthesis characterization and morphological study of $\text{Fe}_3\text{O}_4@\text{SiO}_2$ Core-Shell Nanoparticles. Royal International Global Journal of Advance and Applied Research, 2(12), 274–281. <https://doi.org/10.5281/zenodo.18144900>



Synthesis of $\text{Fe}_3\text{O}_4@\text{SiO}_2$ Core-Shell Nanoparticles:

The composite was synthesized by a slight modification of a method that involves microwave heating of a suspension of the as-prepared nanoparticles in distilled water at a higher temperature. Sodium silicate solution was then added dropwise with continuous stirring and heating. The pH of this mixture was adjusted to the appropriate range, and the reaction mixture was further heated in the microwave oven for a few minutes. The silica coating is crucial for preventing particle aggregation and enhancing the stability of the magnetic nanoparticles. The synthesis of magnetite@silica ($\text{Fe}_3\text{O}_4@\text{SiO}_2$) core-shell nanoparticles was achieved through a modified Stöber method, where a uniform silica (SiO_2) layer is deposited onto the surface of pre-synthesized magnetic nanoparticles as shown in **Figure 1**. To begin the procedure, the nanoparticles were dispersed

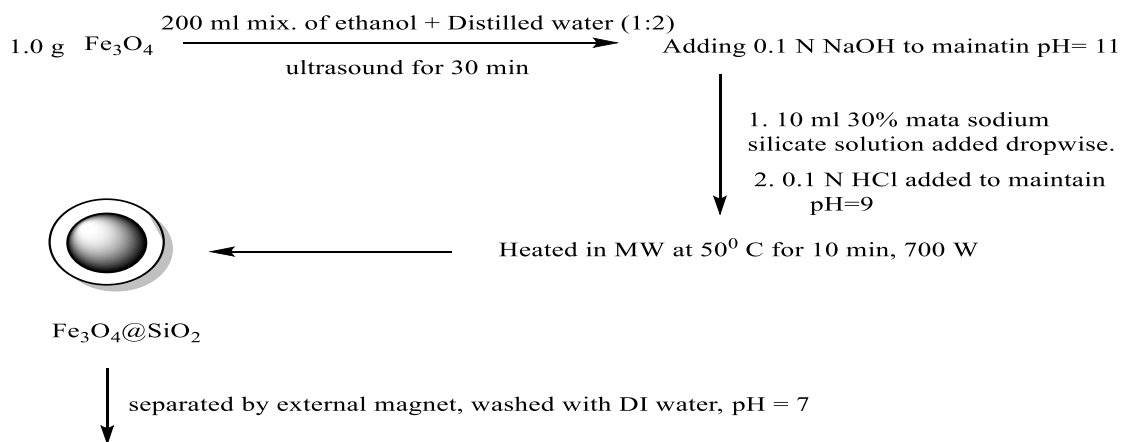
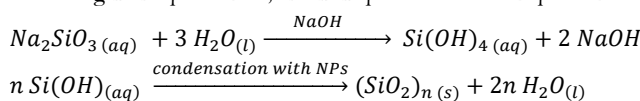


Figure 1 A schematic diagram depicting the synthesis of core-shell nanoparticles using microwave assistance, highlighting the reaction conditions and sequence of processing steps.

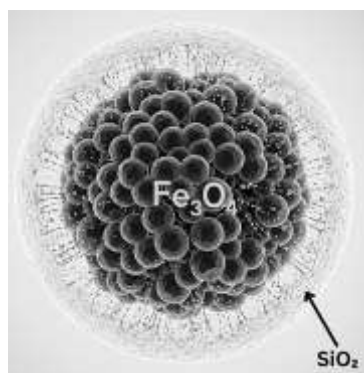


Figure 2 An illustrative representation of nanoparticles featuring a core-shell design, with a magnetic core encased by an outer shell.

The resulting mixture was stirred for one hour and then subjected to microwave irradiation to enhance the density and uniformity of the shell. After overnight aging, the core-shell product was repeatedly washed with deionised water until a neutral pH was achieved, followed by an ethanol wash. The nanoparticles were effectively separated from the solution using an external magnet and dried

overnight in a hot air oven at 80°C to produce a fine powder.

Results and Discussion:

X-ray Diffraction (XRD) Analysis:

XRD recorded on Panalytical's X'Pert Pro, which is indispensable for confirming the crystalline structure, phase purity, and lattice parameters of the synthesized

MOFs and their magnetic components. As depicted in Figure 3, the characteristic diffraction patterns of Fe_3O_4 can be identified. The base nanoparticles displayed a distinct cubic spinel structure, with well-defined diffraction peaks at 2θ values of approximately 30.1° (220), 35.5° (311), 43.1° (400), 57.0° (511), and 62.6° (440). These peaks corresponded to the standard magnetite phase, confirming the successful synthesis of crystalline magnetic nanoparticles. The

prominent diffraction peaks were indexed to align well with the standard JCPDS data for. When silica was coated to form, the magnetite peaks remained at similar positions and relative intensities, suggesting that the silica layer was amorphous and did not disrupt the crystalline structure of the magnetic core. The slight decrease in peak intensities indicates successful surface coating. [9,10].

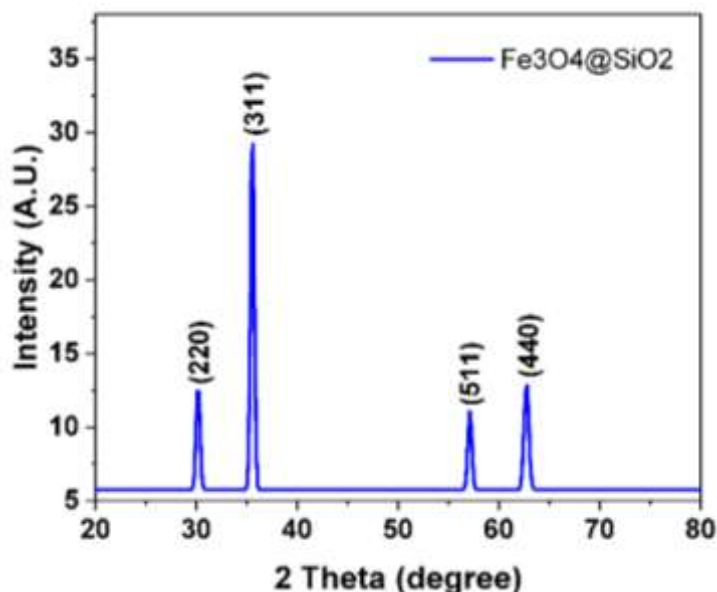


Figure 3 XRD patterns of nanocomposites.

Table 2 X-ray diffraction (XRD) data for $\text{Fe}_3\text{O}_4@\text{SiO}_2$, including Miller indices (hkl), diffraction angles (2θ , θ), interplanar spacing (d), lattice parameter (a), and crystallite size (D) calculated using the Scherrer equation.

Fourier Transform Infrared Spectroscopy (FTIR):

FTIR was taken at SAIF Punjab University on Perkin Elmer - Spectrum RX-IFTIR. FTIR is a critical for identifying the functional groups present in the synthesized

materials, confirming the successful coordination of organic linkers to metal centers, the presence of amino and sulfonic groups, and the formation of Fe-O bonds in the magnetic core. Upon silica coating to form, additional Si-O stretching peaks emerge around 1022-1034, confirming successful surface modification while preserving the magnetic core integrity [11, 12].

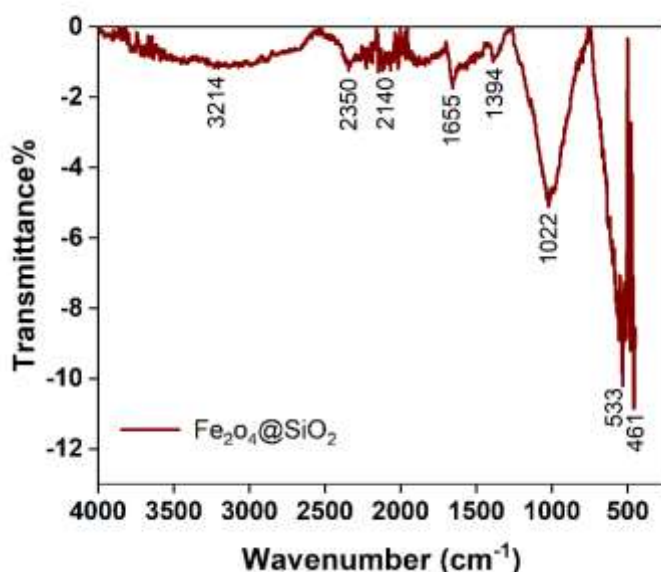


Figure 4 FTIR spectra of nanoparticles

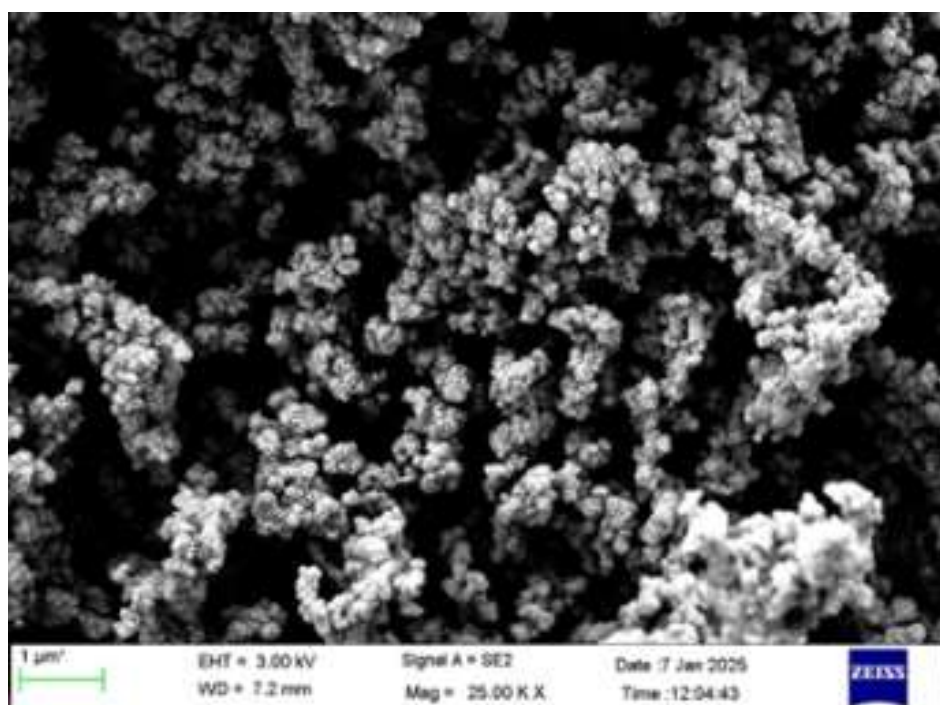


$Fe_3O_4@SiO_2$										
h	k	l	2θ	θ	sinθ	$2sin\theta$	d	(a/d)²	a	D nm
2	2	0	30.1	15.1	0.261	0.522	2.958	8.027	8.366	18.5
3	1	1	35.5	17.8	0.304	0.608	2.523	11.044	8.363	19.8
4	0	0	43.4	21.7	0.374	0.748	2.075	16.242	8.317	20.2
5	1	1	57.1	28.6	0.475	0.950	1.613	27.070	8.369	20.2
4	4	0	62.7	31.4	0.523	1.046	1.478	32.082	8.369	17.1
									8.357	19.2

Fourier Transform Infrared Spectroscopy (FTIR):

Scanning Electron Microscopy (SEM) was utilized to observe the surface morphology, particle size, and overall topography of the synthesized nanoparticles carried out at Jeol 6390LA/ OXFORD XMX N (DST-SAIF Cochin). It provides high-resolution, three-dimensional images, crucial for understanding the shape, size, and

arrangement of particles. As shown in **Figure 5**, the pristine nanoparticles exhibit a relatively uniform spherical morphology with smooth surfaces and particle sizes in the nanometer range. Upon silica coating to form, the particles maintain their spherical shape but show increased surface roughness and slightly larger dimensions due to the silica shell formation [13].

**Figure 5** SEM images of $Fe_3O_4@SiO_2$ nanoparticles**Scanning Electron Microscopy (SEM):**

Utilizing this technique, quantitative data regarding the elemental composition of the synthesized materials was obtained, verifying both the ratios of the constituent elements and the successful functionalization performed at Jeol 6390LA/ OXFORD XMX N (DST-SAIF Cochin), as illustrated in Figure 6. The pristine nanoparticles show characteristic peaks for iron (Fe) and oxygen (O) with the expected stoichiometric ratio, confirming the magnetite phase formation. Upon silica

coating to form, additional silicon (Si) and oxygen peaks appear, indicating successful silica shell deposition while maintaining the underlying iron oxide core signals [14]. The relative peak intensities provide insights into the distribution and loading of each component, with the magnetic core signals being attenuated by the outer layers while maintaining detectability, indicating effective but not complete encapsulation that preserves the composite's multifunctional properties [15, 16].

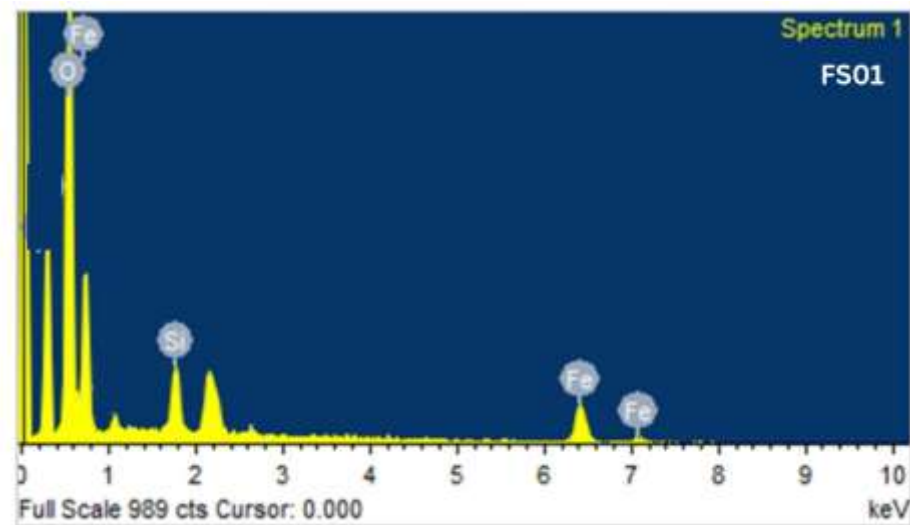


Figure 6 EDX pattern of Fe₃O₄@SiO₂ nanoparticles

Elemental Analysis (EDX)

Transmission Electron Microscopy (TEM) was conducted at SAIF Mumbai, which provides high-resolution images of the internal structure, morphology, and core-shell formation of composite materials. This technique offers detailed insights into particle size and distribution at the nanoscale, distinguishing between surface and internal compositions [17], as illustrated in **Figure 7**. TEM reveals that Fe₃O₄ appears as uniform, spherical nanoparticles,

generally measuring 10-15 nm. The selected area electron diffraction (SAED) patterns displayed distinct rings, confirming their crystalline cubic inverse spinel structure. For, TEM clearly shows a core-shell structure, with a dark core surrounded by a lighter, amorphous silica () shell [18-20]. The SAED pattern supports this observation, showing the crystalline rings of the core along with a diffuse halo from the amorphous silica, as depicted in **Figure 8**.

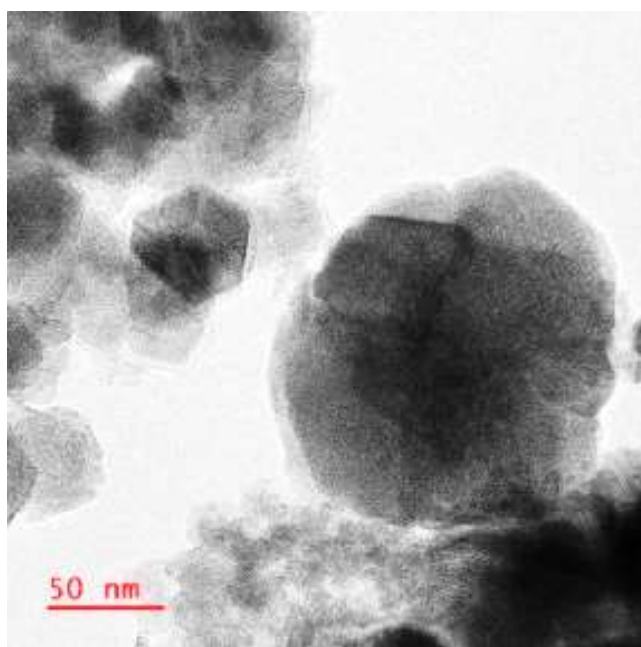


Figure 7. HR-TEM of nanoparticles

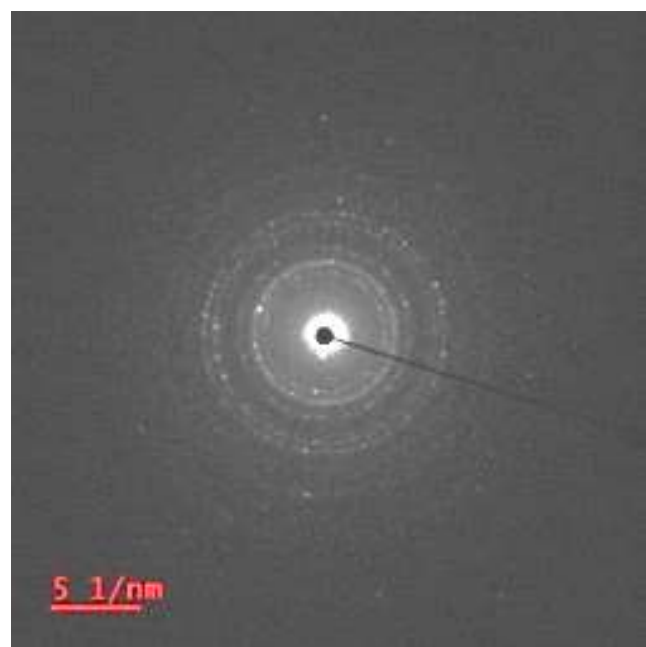


Figure 8. SAED image of nanoparticles

The TEM-derived particle size values range widely across samples, reflecting the influence of different surface functionalizations and composite architectures. The bare Fe₃O₄ nanoparticles exhibited a size of 147.5 nm, which slightly increases to 157.7 nm upon SiO₂ coating, indicating successful shell formation [21, 22].

Table 3 Particle Size (via TEM), zeta potential (mV), and electrophoretic mobility (cm²/Vs) of various synthesized samples including nanoparticles



Sample	Particle size (nm)	Zeta Potential (mV)		Electrophoretic Mobility (cm ² /Vs)	
Fe ₃ O ₄	147.5	-41.4		-0.000321	
Fe ₃ O ₄ @SiO ₂	157.7	-23.5	-38.4	-0.000182	-0.0003

Vibrating Sample Magnetograph (VSM):

VSM was done at at SAIF Mumbai which offers high-resolution imaging of the internal structure, morphology, and core-shell formation of the composite materials, providing detailed information on particle size and distribution at the nanoscale. It can distinguish between surface and internal compositions. The Vibrating Sample Magnetometer (VSM) analysis provides insights into the

magnetic properties of the synthesized materials. At the outset, the nanoparticles demonstrated superparamagnetic behavior, which is indicated by a characteristic S-shaped hysteresis loop with very low remanence and coercivity, and a saturation magnetization (Ms) close to 28 emu/g. Once coated with silica, the core-shell particles exhibit superparamagnetism, with an Ms value of approximately 41 emu/g [23, 24].

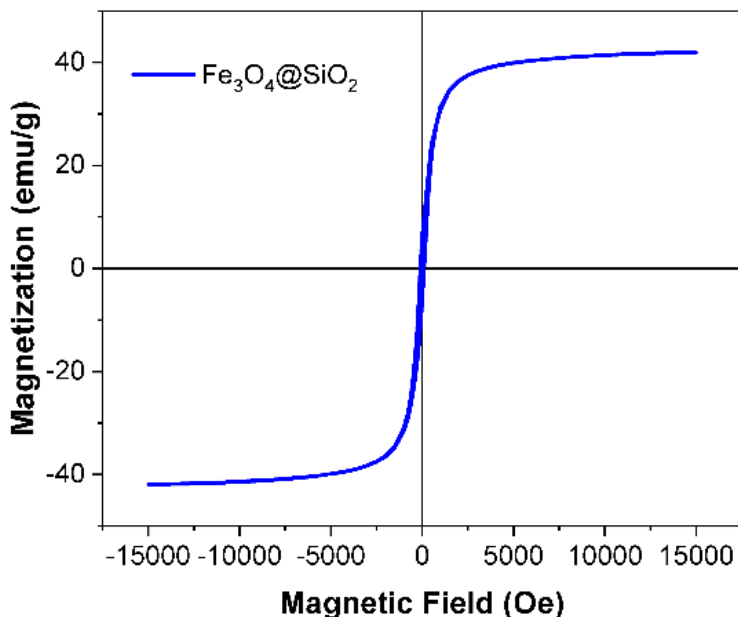


Figure 9 VSM images of nanoparticles

Conclusion:

This study effectively produced and analyzed Fe₃O₄@SiO₂ core-shell nanoparticles through a modified Stöber method enhanced by microwave technology. XRD analysis verified the cubic spinel structure, displaying characteristic diffraction peaks at $2\theta = 30.1^\circ$ (220), 35.5° (311), 43.1° (400), 57.0° (511), and 62.6° (440), with an average crystallite size of 19.2 nm. FTIR spectroscopy identified Si-O stretching peaks between 1022-1034 cm⁻¹, indicating successful silica coating. TEM analysis showed a well-defined core-shell structure, with particle size increasing from 147.5 nm for Fe₃O₄ to 157.7 nm for Fe₃O₄@SiO₂. VSM measurements revealed improved superparamagnetic properties, with saturation magnetization rising from 28 emu/g to 41.0 emu/g following silica coating. The nanoparticles demonstrated excellent colloidal stability, with zeta potential values ranging from -23.5 to -38.4 mV. These findings confirm the successful creation of multifunctional magnetic nanocomposites that maintain crystallinity, exhibit enhanced magnetic properties, and offer superior stability, making them promising for applications in biomedicine, drug

delivery, magnetic separation, catalysis, and environmental clean-up.

Acknowledgment

The authors express their sincere gratitude to all individuals and institutions that contributed directly or indirectly to the successful completion of this research work. Special thanks are extended to Yashwantrao Chavan Maharashtra Open University (YCMOU), Nashik, and Sundarrao More Arts, Commerce and Science College, Poladpur, Raigad, for providing academic support, laboratory facilities, and a conducive research environment. The authors gratefully acknowledge the technical assistance and instrumental support provided by the Sophisticated Analytical Instrumentation Facilities (SAIF) at Punjab University, Chandigarh, SAIF Mumbai, and DST-SAIF Cochin, for FTIR, TEM, VSM, SEM, and EDX analyses. Their expertise and cooperation were invaluable for the successful characterization of the synthesized nanoparticles. Sincere appreciation is also extended to colleagues, research scholars, and faculty members for their constructive discussions, encouragement, and valuable suggestions during the course of this study. The authors acknowledge the contributions of earlier researchers whose published



literature and reference works formed the scientific foundation of this research.

Finally, the authors express heartfelt thanks to family members and well-wishers for their continuous motivation, patience, and moral support throughout the research work.

Financial support and sponsorship

Nil.

Conflicts of interest

The authors declare that there are no conflicts of interest regarding the publication of this paper.

Reference

1. Yang, F., Li, J., Chen, T., Ren, W., Gao, C., Lin, J., Xu, C., Ma, X., Xing, J., Bao, H., Jiang, B., Xiang, L., & Wu, A. (2025). Applications of magnetic nanoparticles for boundaries in biomedicine. *Fundamental Research*, 5(4), 1401–1422. <https://doi.org/10.1016/j.fmre.2024.12.017>
2. Chu, T.-D., Pham, D.-T., Kim, D.-H., Doan, T.-T.-P., Nguyen, T.-S., Nguyen, X.-T., & Quach, D.-T. (2020). Synthesis and Properties of Magnetic-Semiconductor $\text{Fe}_3\text{O}_4/\text{TiO}_2$ Heterostructure Nanocomposites for Applications in Wastewater Treatment. *Journal of Magnetics*, 25(1), 1–7. <https://doi.org/10.4283/jmag.2020.25.1.001>
3. Petrov, K., & Chubarov, A. (2022). Magnetite Nanoparticles for Biomedical Applications. *Encyclopedia*, 2(4), 1811–1828. <https://doi.org/10.3390/encyclopedia2040125>
4. Demirer, G. S., Okur, A. C., & Kizilel, S. (2015). Synthesis and design of biologically inspired biocompatible iron oxide nanoparticles for biomedical applications. *Journal of Materials Chemistry B*, 3(40), 7831–7849. <https://doi.org/10.1039/c5tb00931f>
5. Jungcharoen, P., Pédrot, M., Masson, D., Marsac, R., & Choueikani, F. (2023). Influence of organic ligands on the stoichiometry of magnetite nanoparticles. *Nanoscale Advances*, 5(16), 4213–4223. <https://doi.org/10.1039/d3na00240c>
6. Schwaminger, S., Berensmeier, S., & Syhr, C. (2020). Controlled Synthesis of Magnetic Iron Oxide Nanoparticles: Magnetite or Maghemite? *Crystals*, 10(3), 214. <https://doi.org/10.3390/cryst10030214>
7. Koçak Soylu, S., Özdemir, O. S., Asiltürk, M., & Atmaca, İ. (2025). Thermal and Optical Characteristics of $\text{TiO}_2@\text{SiO}_2$, $\text{Fe}_3\text{O}_4@\text{SiO}_2$, and $\text{ZnO}@\text{SiO}_2$ Core-Shell Nanoparticles and Their Water-Based Nanofluids. *International Journal of Thermophysics*, 46(6). <https://doi.org/10.1007/s10765-025-03558-w>
8. Kharat, Z., Ghavidast, A., Galangash, M., & Shirzad-Siboni, M. (2018). Removal of reactive black 5 dye from aqueous solutions by $\text{Fe}_3\text{O}_4@\text{SiO}_2$ -APTES nanoparticles. *Caspian Journal of Environmental Sciences*, 16(3), 287–301. <https://doi.org/10.22124/cjes.2018.3068>
9. Azarnier, S. G., Esmkhani, M., Dolatkhah, Z., & Javanshir, S. (2022). Collagen-coated superparamagnetic iron oxide nanoparticles as a sustainable catalyst for spirooxindole synthesis. *Scientific Reports*, 12(1). <https://doi.org/10.1038/s41598-022-10102-5>
10. Faaliyan, K., Afghahi, S. S. S., Borhani, E., & Abdoos, H. (2018). Magnetite-silica nanoparticles with core-shell structure: single-step synthesis, characterization and magnetic behavior. *Journal of Sol-Gel Science and Technology*, 88(3), 609–617. <https://doi.org/10.1007/s10971-018-4847-z>
11. Cannas, C., Sanna, R., Musinu, A., Piccaluga, G., Orrù, F., Peddis, D., Angius, F., Ardu, A., Casu, M., & Diaz, G. (2010). CoFe_2O_4 and $\text{CoFe}_2\text{O}_4/\text{SiO}_2$ Core/Shell Nanoparticles: Magnetic and Spectroscopic Study. *Chemistry of Materials*, 22(11), 3353–3361. <https://doi.org/10.1021/cm903837g>
12. Luo, P., Yu, H., Yang, L., Yuan, H., Wang, C., Liu, Z., Wu, W., & Wang, Y. (2023). Properties Optimization of Soft Magnetic Composites Based on the Amorphous Powders with Double Layer Inorganic Coating by Phosphating and Sodium Silicate Treatment. *Metals*, 13(3), 560. <https://doi.org/10.3390/met13030560>
13. Zhi, D., Wang, H., Jiang, D., Parkin, I. P., & Zhang, X. (2019). Reactive silica nanoparticles turn epoxy coating from hydrophilic to super-robust superhydrophobic. *RSC Advances*, 9(22), 12547–12554. <https://doi.org/10.1039/c8ra10046b>
14. Zaytseva, M. P., Grebenников, I. S., Muradova, A. G., Savchenko, A. G., Sharapaev, A. I., & Yurtov, E. V. (2018). $\text{Fe}_3\text{O}_4/\text{SiO}_2$ Core Shell Nanostructures: Preparation and Characterization. *Russian Journal of Inorganic Chemistry*, 63(12), 1684–1688. <https://doi.org/10.1134/s0036023618120239>
15. Post, P., Wurlitzer, L., Maus-Friedrichs, W., & Weber, A. P. (2018). Characterization and Applications of Nanoparticles Modified in-Flight with Silica or Silica-Organic Coatings. *Nanomaterials*, 8(7), 530. <https://doi.org/10.3390/nano8070530>
16. Husain, H., Sulthonul, M., Hariyanto, B., Klysubun, W., Pratapa, S., & Darminto, D. (2019). Structure and magnetic properties of silica-coated magnetite-nanoparticle composites. *Materials Research Express*, 6(8), 086117. <https://doi.org/10.1088/2053-1591/ab29af>
17. Torres-Gómez, N., Argueta-Figueroa, L., García-Contreras, R., Vilchis-Nestor, A. R., Baeza-Barrera, A., & Nava, O. (2019). Shape Tuning of Magnetite Nanoparticles Obtained by Hydrothermal Synthesis: Effect of Temperature. *Journal of Nanomaterials*, 2019, 1–15. <https://doi.org/10.1155/2019/7921273>
18. Abbas, M., Chen, J., & Abdel-Hamed, M. O. (2017). Efficient one-pot sonochemical synthesis of thickness-controlled silica-coated superparamagnetic iron oxide ($\text{Fe}_3\text{O}_4/\text{SiO}_2$) nanospheres. *Applied Physics A*, 123(12). <https://doi.org/10.1007/s00339-017-1397-0>
19. Lin, C.-R., Ivanova, O. S., Petrov, D. A., Sokolov, A. E., Chen, Y.-Z., Gerasimova, M. A., Zharkov, S. M., Tseng, Y.-T., Shestakov, N. P., & Edelman, I. S. (2021). Amino-Functionalized $\text{Fe}_3\text{O}_4@\text{SiO}_2$ Core-Shell Magnetic Nanoparticles for Dye Adsorption. *Nanomaterials*, 11(9), 2371. <https://doi.org/10.3390/nano11092371>
20. Ansari, S. M., Ghosh, K. C., Kolekar, Y. D., Sen, D., Devan, R. S., Sastry, P. U., & Ramana, C. V. (2020).



Eco-Friendly Synthesis, Crystal Chemistry, and Magnetic Properties of Manganese-Substituted CoFe_2O_4 Nanoparticles. *ACS Omega*, 5(31), 19315–19330. <https://doi.org/10.1021/acsomega.9b02492>

21. Albutt, N., Sonsupup, S., Thonglor, P., & Sinprachim, T. (2024). Synthesis of Magnetic Nanoparticles Coated with Chitosan for Biomedical Applications. *Key Engineering Materials*, 1005, 49–57. <https://doi.org/10.4028/p-9xdpmd>

22. Dabagh, S., & Dini, G. (2019). Synthesis of Silica-Coated Silver-Cobalt Ferrite Nanoparticles for Biomedical Applications. *Journal of Superconductivity and Novel Magnetism*, 32(12), 3865–3872. <https://doi.org/10.1007/s10948-019-05172-y>

23. Husain, H., Sulthonul, M., Hariyanto, B., Klysubun, W., Pratapa, S., & Darminto, D. (2019). Structure and magnetic properties of silica-coated magnetite-nanoparticle composites. *Materials Research Express*, 6(8), 086117. <https://doi.org/10.1088/2053-1591/ab29af>

24. Shen, L., Song, J., Qiao, Y., & Li, B. (2019). Monodisperse $\text{Fe}_3\text{O}_4/\text{SiO}_2$ and $\text{Fe}_3\text{O}_4/\text{SiO}_2/\text{PPy}$ Core-Shell Composite Nanospheres for IBU Loading and Release. *Materials*, 12(5), 828. <https://doi.org/10.3390/ma12050828>